Hall Effect

Appendix A

Theory and Description of Experiment

Source: “Experiments in Modern Physics (First Ed.), A.C. Melissinos”

and for Stefan's constant, $\sigma = 2.7 \times 10^{-8}$ joules m^{-2} deg^{-4} sec^{-1} which is of the correct order of magnitude, and smaller† than σ.

In concluding, we note that our results have confirmed the exponential dependence on temperature of the thermionic current (Richardson's equation), and the phenomena of space charge. Also, qualitative agreement has been achieved with the accepted values of the parameters involved; similarly, agreement has been achieved for Stefan's law.

3. Some Properties of Semiconductors

3.1 General

We have seen in the first section how a free-electron gas behaves, and what can be expected for the band structure of a crystalline solid. In the second section we applied the principle of free-electron gas behavior to the emission of electrons from metals, and in the present section we will apply both principles to the study of some properties of semiconductors which can be verified easily in the laboratory.

As mentioned before, a semiconductor is a crystalline solid in which the conduction band lies close to the valence band, but is not populated at low temperatures; semiconductors are unlike most metals in that both *electrons* and *holes* are responsible for the properties of the semiconductor. If the semiconductor is a pure crystal, the number of holes (positive carriers, p) is equal to the number of free electrons (negative carriers, n), since for each electron raised to the conduction band, a hole is created in the valence band; these are called the *intrinsic* carriers.

All practically important semiconductor materials, however, have in them a certain amount of impurities which are capable either of donating electrons to the conduction band (making an n-type crystal) or of accepting electrons from the valence band, thus creating holes in it (making a p-type crystal). These impurities are called *extrinsic* carriers; in such crystals $n \neq p$.

Let us then first look at the energy-band picture of a semiconductor as it is shown in Fig. 3.18; the impurities are all concentrated at a single energy level usually lying close to, but below, the conduction band. The density of states has to be different from that of a free-electron gas (Eq. 1.4 and Fig. 3.2a) since, for example, in the forbidden gaps it must be zero; close to the ends of the allowed bands it varies as $E^{1/2}$ and reduces to zero on the edge. On the other hand, the Fermi distribution function, Eq. 1.3, remains the same. The only parameter in this function is the Fermi energy, which can be found by integrating the number of *occupied* states (Fermi function

† Note that the tungsten filament is not a perfect black body; the emissivity of a hot tungsten filament is usually taken as one third.

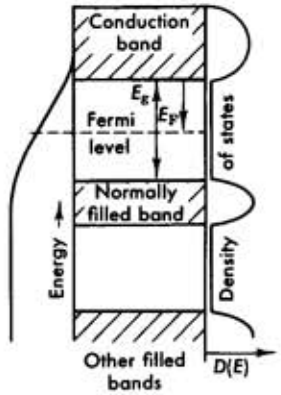

FIG. 3.18 Energy band structure of a semiconductor without impurities. On the left-hand side the Fermi distribution for a free-electron gas is shown; on the right-hand side the actual density of states $D(E)$ is shown.

times density of states) and setting it equal to the electron density. It is clear, however, that if we are to have as many empty states in the valence band as occupied ones in the conduction band, the Fermi level must lie exactly in the middle of the forbidden gap† (because of the symmetry of the trailing edge of the distribution). In Fig. 3.18, the density of states is shown to the right and the Fermi distribution function to the left. We measure the position of the Fermi level *from the conduction band* and define it by E_F; the exact value of E_F is

$$E_F = -\frac{E_g}{2} + kT \ln \left(\frac{m_h^*}{m_e^*}\right)^{3/4} \tag{3.1}$$

Since the Fermi level lies below the conduction band, E_F is a *negative* quantity; E_g is the energy gap always taken positive and m_h^* and m_e^* are the effective masses of holes and electrons, respectively. If w_C and w_F stand for the actual position of the conduction band and Fermi level above the zero point energy, then

$$w_F = w_C + E_F$$

To find the number of electrons in the conduction band (or holes in the valence band) we simply substitute Eq. 3.1 for w_F into Eq. 1.4, multiply by the density of states, and integrate over w from $w = w_C$ to $+\infty$. When, however, the exponent

$$-(w_F - w) \approx \frac{E_g}{2} + E \gg kT \tag{3.2}$$

the Fermi distribution degenerates to a Boltzmann distribution. (Here E is the energy of the electrons as measured from the top of the conduction band; obviously it can take either positive or negative values.) With this

† If the effective masses of p- and n-type carriers are the same.

assumption the integration is easy, yielding

$$n = \left(\frac{2\pi m_e kT}{h^2}\right)^{3/2} e^{E_F/kT} \simeq \left(\frac{2\pi m_e kT}{h^2}\right)^{3/2} e^{-E_g/2kT} \tag{3.3a}$$

similarly,

$$p = \left(\frac{2\pi m_h kT}{h^2}\right)^{3/2} e^{-(E_g+E_F)/kT} \simeq \left(\frac{2\pi m_h kT}{h^2}\right)^{3/2} e^{-E_g/2kT} \tag{3.3b}$$

It is interesting that the product np is independent of the position of the Fermi level†—especially if we take $m_e = m_h$

$$n_i^2 = np = 2.31 \times 10^{31}\, T^3\, e^{-E_g/kT}$$

Thus it should be expected that as the temperature is raised, the intrinsic carriers of a semiconductor will increase at an exponential rate characterized by $E_g/2kT$. This temperature is usually very high since $E_g \approx 0.7$ V (see Eqs. 3.5).

We have already mentioned that impurities determine the properties of a semiconductor, especially at low temperatures where very few intrinsic carriers are populating the conduction band. These impurities, when in their ground state, are usually concentrated in a single energy level lying very close to the conduction band (if they are donor impurities) or very close to the valence band (if they are acceptors). As for the intrinsic carriers, the Fermi level for the impurity carriers lies halfway between the conduction (valence) band and the impurity level; this situation is shown in Figs. 3.19a and 3.19b. If we make again the low temperature approximation of Eq. 3.2, the number of electrons in the conduction band is given by

$$n = N_d \left(\frac{2\pi mkT}{h^2}\right)^{3/2} e^{-E_d/2kT} \tag{3.4}$$

where N_d is the number of donors and E_d the separation of the donor energy level from the conduction band. In writing Eq. 3.4, however, care must be exercised because the conditions of Eq. 3.2 are valid only for very low temperatures. Note, for example, that for germanium

$$E_g = 0.7 \text{ eV}, \qquad \text{and for } kT = 0.7 \text{ eV}, \qquad T = 8{,}000^\circ \text{ K}$$

whereas

$$E_d = 0.01 \text{ eV}, \qquad \text{and for } kT = 0.01 \text{ eV}, \qquad T = 120^\circ \text{ K} \tag{3.5}$$

Thus at temperatures $T \gtrsim 120^\circ$ K most of the donor impurities will be

† This result is very general and holds even without the approximation that led to Eqs. 3.3.

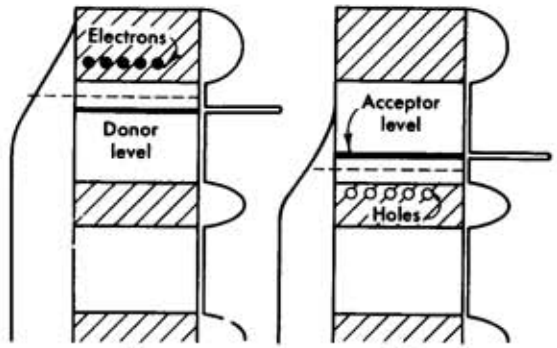

FIG. 3.19 Same as Fig. 3.18 but with the addition of impurities. (a) The impurities are of the donor type and lie at an energy slightly below the conduction band. (b) The impurities are of the acceptor type and lie slightly above the valence band. Note the shift of the Fermi level as indicated by the dotted line.

in the conduction band and instead of Eq. 3.4 we will have $n \simeq N_d$; namely, the number of impurity carriers becomes saturated. Once saturation has been reached the impurity carriers in the conduction band behave like the free electrons of a metal.

In the experiments to be discussed below, the lowest temperature achieved was $T \simeq 84^\circ$ K; for germanium this still corresponds to almost complete saturation of the impurity carriers. We will, however, be able to study the gradual increase, as a function of the temperature, of the *intrinsic* carriers of germanium.

3.2 RESISTIVITY

We know already that conduction in solids is due to the motion of the charge carriers under the influence of an applied field. We define the following symbols:

$\mathbf{J}$ = current density
σ = conductivity, such that $\sigma\mathbf{E} = \mathbf{J}$; $\rho = 1/\sigma$ = resistivity
e = charge of the electron
n = (negative) carrier density; p = (positive) carrier density
$\bar{v}$ = drift velocity
$\mathbf{E}$ = applied electric field
μ = mobility; such that $\mu\mathbf{E} = \bar{\mathbf{v}}$.
m^* = effective mass; m_e^*, m_h^* for electrons, holes
λ = mean free path between collisions

From simple reasoning, the current density is

$$e \times \text{(number of carriers traversing unit area in unit time)}$$

which is equivalent to the carrier density multiplied by the drift velocity. Thus

$$\mathbf{J} = \mathbf{I}/A = e(n\bar{\mathbf{v}}_e - p\bar{\mathbf{v}}_h) \tag{3.6}$$

however, if s is the distance traveled and t the time between thermal collisions,

$$s = \frac{1}{2}\alpha t^2 = \frac{1}{2}\frac{e\,|\,\mathbf{E}\,|}{m^*}t^2$$

and

$$\bar{v} = \frac{s}{t} = \frac{1}{2}\frac{e\,|\,\mathbf{E}\,|}{m^*}t$$

in terms of the mean free path, $t = \lambda/v$, where v is now the thermal velocity,

$$\frac{m^*v^2}{2} = \frac{3}{2}kT$$

thus

$$\bar{\mathbf{v}} = \frac{e\lambda\mathbf{E}}{2\sqrt{3kTm^*}}$$

If only one type of carrier is present,

$$\mathbf{J} = en\bar{\mathbf{v}} = en\mu\mathbf{E}$$

and

$$\sigma = en\mu = \frac{ne^2\lambda}{2\sqrt{3kTm^*}}$$

Thus, if (a) the number of carriers is constant, and (b) the mean free path remains constant, the conductivity should decrease as $T^{-1/2}$. The first of these conditions holds in the extrinsic region after all impurity carriers are in the conduction band; the mean free path, however, is not constant, because higher temperatures increase lattice vibrations, which in turn affect the scattering of the carriers. A simple calculation suggests a $1/kT$ dependence for λ, so that

$$\sigma = ne\mu = C\frac{ne^2}{m^*}T^{-3/2} \tag{3.7}$$

where C is a constant. We will see that this dependence is not always observed experimentally.

3.3 The Hall Effect

It is clear from Eq. 3.6 that conductivity measurements cannot reveal whether one or both types of carriers are present, nor distinguish between them. However, this information can be obtained from Hall effect measurements, which are a basic tool for the determination of mobilities. The effect was discovered by E. H. Hall in 1879.

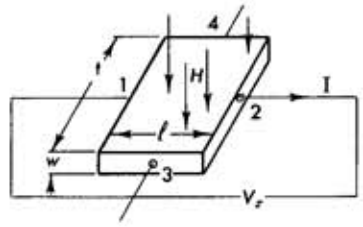

Fig. 3.20 Schematic arrangement for the measurement of the Hall effect of a crystal.

Consider a simple crystal mounted as in the Fig. 3.20, with a magnetic field H in the z direction perpendicular to contacts 1, 2 and 3, 4. If current is flowing through the crystal in the x direction (by application of a voltage V_x between contacts 1 and 2), a voltage will appear across contacts 3, 4. It is easy to calculate this (Hall) voltage if it is assumed that all carriers have the same drift velocity. We will do this in two steps: (a) by assuming that carriers of only one type are present, and (b) by assuming that carriers of both types are present.

(*a*) *One type of carrier.* The magnetic force on the carriers is $\mathbf{F}_m = e(\bar{\mathbf{v}} \times \mathbf{H})$ and it is compensated by the Hall field $\mathbf{F}_H = e\mathbf{E}_H = eE_y\mathbf{i}_y$ thus $\bar{v}H = E_y$, but $\bar{v} = \mu E_x$, hence $E_y = H\mu E_x$. The Hall coefficient R_H is defined as

$$|\,R_H\,| = \frac{E_y}{J_xH} = \frac{\mu E_x}{J_x} = \frac{\mu}{\sigma} = \frac{1}{ne} \tag{3.8a}$$

Hence for fixed magnetic field and fixed *input current*, the Hall voltage is proportional to $1/n$. It follows that

$$\mu_H = R_H\sigma, \tag{3.8b}$$

providing an experimental measurement of the mobility; R_H is expressed in cm^3 coulomb^{-1}, and σ in ohm^{-1} cm^{-1}; thus μ is expressed in units of cm^2 volt^{-1} sec^{-1}.

In most experiments the voltage across the input is kept constant, so that it is convenient to define the Hall angle as the ratio of applied and measured voltages:

$$\phi = \frac{V_y}{V_x} = \frac{E_yt}{E_xl} = \mu\frac{t}{l}H \tag{3.8c}$$

where l is the length and t the thickness of the crystal.

The Hall angle is proportional to the mobility, and

$$\rho V_y = \left(\frac{t}{l} H\right) \frac{1}{ne} \tag{3.9}$$

is again proportional to $1/n$ and thus to $| R_H |$.

(*b*) *Two types of carriers.* Now it is important to recognize that for the same electric field E_x, the Hall voltage for p carriers will have opposite sign from that for n carriers. (That is, the Hall coefficient R has a different sign.) Thus, the Hall field E_y will not be able to compensate for the magnetic force on both types of carriers and there will be a transverse motion of carriers; however, the net transverse transfer of charge will remain zero since there is no current through the 3, 4 contacts; this statement is expressed as

$$e(v_y^+ n - v_y^- n) = 0$$

while

$$e(v_x^+ n - v_x^- p) = J_x \qquad \text{and} \qquad e(\mu^+ p + \mu^- n) = \sigma$$

where the mobility is always a positive number; however, v_x^+ has the opposite sign from v_x^-, but

$$v_y = \frac{s}{t} = \left(\frac{1}{2} \frac{F}{m^*} t^2\right) \frac{1}{t}$$

where

$$\mathbf{F}^+ = e[(\mathbf{v}_x^+ \times \mathbf{H}) - \mathbf{E}_y]$$

$$\mathbf{F}^- = -e[(\mathbf{v}_x^- \times \mathbf{H}) - \mathbf{E}_y]$$

Thus

$$v_y^+ = \frac{1}{2} \frac{e}{m_h^*} t[(\mu^+ E_x H) - E_y] = \mu^+(\mu^+ E_x H - E_y)$$

$$v_y^- = \frac{1}{2} \frac{e}{m_e^*} t[(\mu^- E_x H) - E_y] = \mu^-(\mu^- E_x H + E_y)$$

and thus

$$\mu^+ p(\mu^+ E_x H - E_y) - \mu^- n(\mu^- E_x H + E_y) = 0$$

$$E_y = E_x H \frac{(\mu_h^2 p - \mu_e^2 n)}{\mu_h p + \mu_e n}$$

and for the Hall coefficient R_H

$$R_H = \frac{E_y}{J_x H} = \frac{E_y}{\sigma E_x H} = \frac{\mu_h^2 p - \mu_e^2 n}{e(\mu_h p + \mu_e n)^2} \tag{3.10}$$

Equation 3.10 correctly reduces to Eq. 3.8 when only one type of carrier is present.†

Since the mobilities μ_h and μ_e are not constants but functions of T, the Hall coefficient given by Eq. 3.10 is also a function of T and it may become zero and even change sign. In general $\mu_e > \mu_h$ so that inversion may happen only if $p > n$; thus "Hall coefficient inversion" is characteristic only of "p-type" semiconductors.

At the point of zero Hall coefficient, it is possible to determine the ratio of mobilities $b = \mu_e/\mu_h$ in a simple manner. Since $R_H = 0$, we have from Eq. 3.10

$$nb^2 - p = 0 \tag{3.11}$$

Let N_a be the number of impurity carriers for this "p-type" material; then in the extrinsic region

$$p = N_a \qquad n = 0$$

whereas in the intrinsic region

$$p = N_a + N \qquad n = N$$

and Eq. 3.11 becomes

$$n = \frac{N_a}{b^2 - 1} \tag{3.12}$$

We can also express the conductivity σ at the inversion point, $T = T_0$, in terms of the mobilities

$$\sigma_0 = e[\mu_e n + \mu_h(N_a + n)] \tag{3.13}$$

and this value can be directly measured. Further, by extrapolating conductivity values *from* the extrinsic region to the point $T = T_0$ we obtain

$$\sigma_e(T = T_0) = e\mu_h N_a(T = T_0).$$

It therefore follows that

$$\frac{\sigma_0}{\sigma_e(T = T_0)} = \frac{N_a + n(1 + b)}{N_a} \tag{3.14}$$

† Both Eq. 3.8 and Eq. 3.10 have been derived on the assumption that all carriers have the same velocity; this is not true; but the exact calculation modifies the results obtained here by a factor of only $3\pi/8$.

Substituting the value of n from Eq. 3.12 we obtain

$$\frac{\sigma_0}{\sigma_e} = \frac{b}{b-1}$$

or

$$b = \frac{R_e(T = T_0)}{R_e(T = T_0) - R_0} \tag{3.15}$$

where R_0 is the measured resistance of the sample at the inversion point and $R_e(T = T_0)$ is the resistance extrapolated from the extrinsic region to the value it would have at the inversion temperature (see Fig. 3.27).

We thus see that the Hall effect, in conjunction with resistivity measurements, can provide information on carrier densities, mobilities, impurity concentration, and other values. It must be noted, however, that mobilities obtained from Hall effect measurements $\mu_H = |R_H|\sigma$ do not always

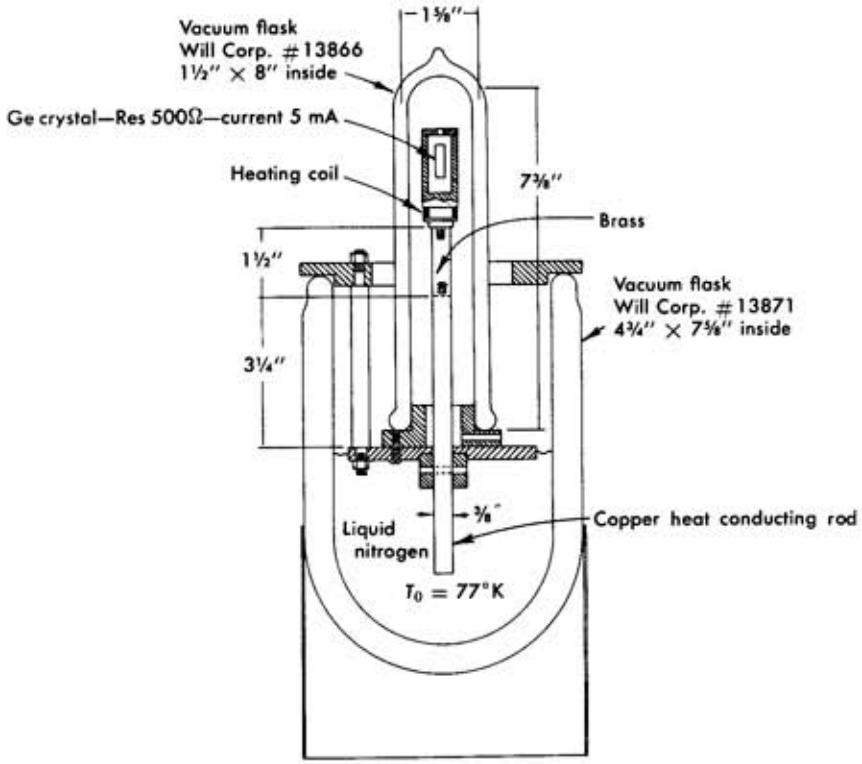

FIG. 3.21 Cryostat and assembly of equipment for Hall effect and resistivity measurements. The dewar is filled with liquid nitrogen; the crystal is mounted on top of a copper rod, which is in contact with the liquid nitrogen.

agree with directly measured values, and a distinction between the two is made; this will become clear when the experimental data are analyzed (Eq. 3.18 and Eq. 3.19).

3.4 Experimental Arrangement and Procedure

The sample, a small crystal of germanium, is mounted in a cryostat; a drawing of the assembly is shown in Fig. 3.21. The small dewar placed on the top permits the use of a magnet with only a 2-in. poleface separation. The heat is drawn from the sample chamber through the copper-brass rod into the liquid nitrogen heat sink. This allows the sample chamber to reach approximately 80° K. The liquid nitrogen must be kept up to level throughout the entire experiment. To raise the temperature of the sample chamber, a heating coil is placed just below it. The coil is wound noninductively of 9 ft of No. 32 cotton-covered resistance wire; between each layer of the winding, metal foil is placed to conduct the heat quickly to the copper chamber. The maximum current is 1.5 amp and the heating coil should not be operated without liquid nitrogen in the large dewar (the maximum current with no liquid nitrogen is 35 ma.). At a current of about 1.3 amp the chamber will be at room temperature.

To measure the temperature, a copper-constantan thermocouple is fastened to the outside of the sample chamber. The standard junction is in ice-water at 0° C and Fig. 3.22 gives the appropriate calibration on this basis.

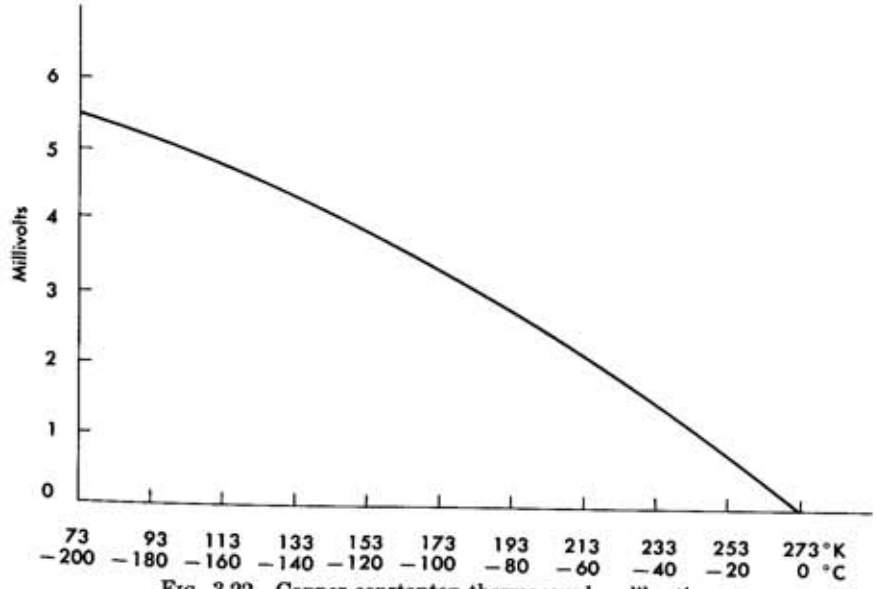

FIG. 3.22 Copper-constantan thermocouple calibration.

The equilibrium time is of the order of 15 min; however, it is not necessary to wait this long between points when taking data. Measurements should start at the lowest temperature, and during the experiment the heating coil current should be kept slightly in advance of equilibrium so as to maintain a slow but steady rise in temperature; the average millivolt reading should be recorded.

One method of mounting the crystal and making the contacts (used in this laboratory) is shown in Fig. 3.23. The copper stub used for one of the sample current contacts also provides a low-resistance heat path to keep the germanium at the sample chamber's temperature. The two wires soldered on each side of the germanium crystal allow the measurement of the Hall voltage at the top or bottom of the sample and the measurement of the conductivity on either side of the sample. Use of fine wires provides isolation from room temperature. The finite extent of the side contacts does not, to first order, affect the conductivity measurements.

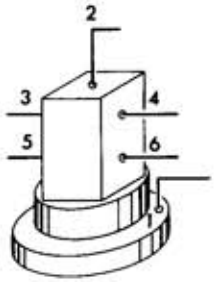

FIG. 3.23 Mounting and electrical connections to a crystal sample.

There are two problems in making the solder contacts. One is wetting the germanium with solder (that is, making the solder contact stick) and the other is to avoid making a "rectifying junction." To wet the germanium it is necessary first to etch it for about 30 sec in a solution of three parts hydrofluoric acid, three parts glacial acetic acid, and four parts nitric acid; this is called the CP4 etching solution. To avoid making a rectifying junction, the surface of the germanium where the contact is to be made must be destroyed; this is best done with a small Swiss file. A colloidal mixture of acid flux and solder is then used (it looks like a gray paste and is called "plumber's solder"). A very quick etch after the contacts have been made helps to remove any flux which would change the conductivity measurements. After etching, the germanium should be handled only with clean tweezers.

A schematic diagram of the measuring circuits is shown in Fig. 3.24. Resistivity is usually measured across contacts 1, 2 and an a-c bridge should be used; this is a more accurate measurement and also reduces the

effects of rectifying contacts. There are provisions to rveerse the sample current, to measure the Hall voltage at either the top or bottom of the sample, and to balance out the zero field potential. The zero field potential comes from two sources: the first is due to the fact that the Hall contacts are not quite opposite each other; since there is a potential gradient due to the sample current, a part of this gradient will be seen between the two contacts. The second source is from the contact potential and the "rectifying action" of the contacts. To measure the Hall voltage, a Keithley electrometer is used, since its high input impedance does not affect the Hall voltage; the sample current is provided from a d-c battery, hence at fixed voltage. The Hall voltage must be measured for both directions of the magnetic field and should always be properly zeroed when the field is off; before the voltage is measured, the crystal must be rotated in the field until the position of maximum voltage is reached.

An experienced experimenter can take all the necessary data in one run. The sample is usually cooled to liquid nitrogen and then the temperature is slowly raised by control of the heater current. The following data should

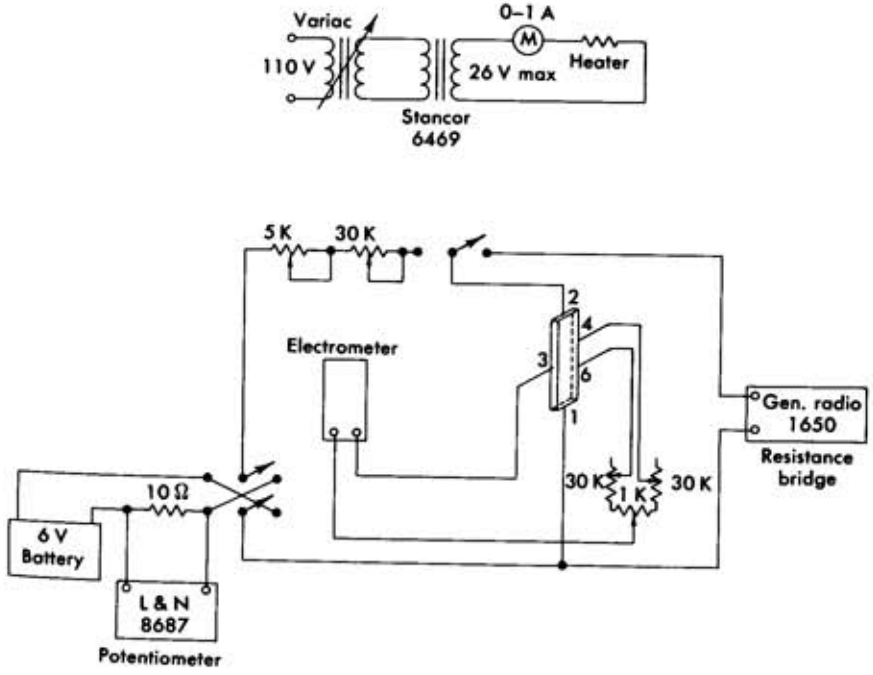

FIG. 3.24 Circuit for measuring conductivity and Hall coefficient of a crystal.

be recorded for every temperature point:

(a) Thermocouple reading
(b) Resistivity; magnetic field off
(c) Resistivity; magnetic field on
(d) Hall voltage, with field forward, off, reversed
(e) Thermocouple reading

Less experienced persons are better advised first to make a measurement of the resistivity only, over the whole temperature range from 80° K to 330° K, and then to measure the Hall voltage separately; as usual, it is advisable to plot the data as it is obtained so as to know where a greater density of measurements is desirable.

3.5 Analysis of Data

Data on Hall effect and resistivity, obtained by students† using a low impurity germanium crystal, are presented and analyzed below.

Table 3.2 gives the raw data; the dimensions of the crystal were $l = 1.09$, $t = 0.183$, $w = 0.143$ cm (see Fig. 3.20). A fixed voltage of 1.32 V was applied across the long end of the sample, and the magnetic field was (800 ± 40) gauss. The Hall voltage was measured across the t dimension of the crystal.

From the data of the Table 3.2 the following plots were made:

(a) $\rho = 1/\sigma = RA/l$, hence‡ $\rho = R \times 2.42 \times 10^{-2}$ ohms-cm; this is shown in a semilog plot against $1/T$ in Fig. 3.25. We note that for $T < 290°$ K, conduction is due mainly to the impurity carriers: this is the *extrinsic region*. For $T > 280°$ K, electrons are transferred copiously from the valence band into the conduction band and the crystal is in the *intrinsic region*. From the slope of the intrinsic region and making use of Eq. 3.3b, we have $\rho \propto 1/n \propto \exp(E_g/2kT)$ and thus $\ln \rho = E_g/2kT$. Hence

$$\frac{E_g}{2k} = \frac{\Delta \log_{10}}{\Delta(1/T)} \frac{1}{\log_{10} e} = \frac{1.81 \times 10^3}{0.4343} \tag{3.16}$$

which leads to $E_g = 0.72 \pm 0.07$ eV, in agreement with the accepted value.

(b) A log-log plot of the resistivity in the extrinsic region against $1/T$ shown in Fig. 3.26. If a power law as in Eq. 3.7 is applicable, we would have $\rho \propto (1/T)^\alpha$ and hence

$$\alpha = \frac{\Delta \log \rho}{\Delta \log (1/T)} = -2.0 \pm 0.1 \tag{3.17}$$

† E. Yadlowski and P. Schreiber, class of 1962.
‡ Note that here R is the resistance of the sample and not the Hall coefficient R_H.

TABLE 3.2
Data on Hall Effect and Resistivity Measurements of Germanium

V_H (Volts) Hall voltage	R_m (Ohms) Magneto-resistance	R (Ohms) Resistance	T_{ms} (millivolts) Thermocouple	T (°K)
0.05 ± 0.002	157.8 ± 0.2	142.0 ± 0.2	5.37	84
0.047 ± 0.002	172.0 ± 0.2	152.0 ± 0.2	5.28	86
0.041 ± 0.002	183.9 ± 0.2	168.0 ± 0.2	5.20	93
0.038 ± 0.002	200.0 ± 0.2	184.9 ± 0.2	5.10	100
0.038 ± 0.002	207.0 ± 0.1	192.0 ± 0.2	5.036	103
0.0375 ± 0.002	219.0 ± 0.2	202.2 ± 0.1	5.00	105
0.0360 ± 0.002	229.0 ± 0.2	215.0 ± 0.4	4.94	111
0.0340 ± 0.002	238.0 ± 0.2	226.0 ± 0.4	4.86	114
0.0330 ± 0.002	261.0 ± 0.2	247.0 ± 0.1	4.78	121
0.0300 ± 0.002	290.0 ± 0.2	276.0 ± 0.2	4.65	127
0.0280 ± 0.002	321.0 ± 0.2	306.0 ± 0.5	4.53	131
0.0275 ± 0.002	335.0 ± 0.5	321.0 ± 0.5	4.45	137
0.0230 ± 0.002	371.0 ± 0.5	360.0 ± 0.5	4.30	143
0.0230 ± 0.002	407.0 ± 0.5	396.0 ± 1	4.15	150
0.0208 ± 0.002	457.5 ± 0.5	446.0 ± 1	3.95	155
0.0204 ± 0.002	495.0 ± 0.5	482.5 ± 2	3.84	164
0.0185 ± 0.001	559.0 ± 0.5	550.0 ± 1	3.60	172
0.0180 ± 0.001	610.0 ± 0.5	595.0 ± 2	3.40	182
0.0145 ± 0.0005	702.0 ± 1	700.0 ± 1	3.10	193
0.0150 ± 0.0005	827.0 ± 2	820.0 ± 1	2.72	199
0.0144 ± 0.0003	855.0 ± 1	850.0 ± 1	2.60	203
0.0131 ± 0.0003	888.0 ± 1	875.0 ± 1	2.45	212
0.0115 ± 0.0003	955.0 ± 1	950.0 ± 1	2.20	241
0.0095 ± 0.0001	1270.0 ± 5	1270.0 ± 5	1.20	253
0.0075 ± 0.0002	1440.0 ± 3	1440.0 ± 3	0.69	262
0.0059 ± 0.0002	1500.0 ± 3	1500.0 ± 3	0.45	260
0.0065 ± 0.0002	1460.0 ± 3	1450.0 ± 5	0.65	263
0.0075 ± 0.0002	1500.0 ± 3	1500.0 ± 4	0.380	266
0.0075 ± 0.0002	1570.0 ± 3	1560.0 ± 6	0.180	270
0.0067 ± 0.0002	1650.0 ± 3	1645.0 ± 5	0.000	273
0.0061 ± 0.0002	1700.0 ± 5	1700.0 ± 5	−0.400	282
0.0055 ± 0.0002	1660.0 ± 5	1665.0 ± 5	−0.630	286
0.0050 ± 0.0002	1610.0 ± 5	1590.0 ± 5	−0.860	290
0.0038 ± 0.0001	1455.0 ± 5	1440.0 ± 5	−1.10	296
0.0032 ± 0.0001	1340.0 ± 5	1310.0 ± 5	−1.22	302
0.0018 ± 0.0001	980.0 ± 5	950.0 ± 5	−1.44	305
0.0008 ± 0.0001	795.0 ± 3	785.0 ± 2	−1.67	312
0.00035 ± 0.00005	654.0 ± 2	632.0 ± 1	−1.86	315
0.00001 ± 0.00002	566.0 ± 2	545.0 ± 1	−2.00	318
0.00000 ± 0.000050	505.0 ± 1	488.0 ± 2	−2.15	323
−0.0002 ± 0.000050	395.0 ± 2	390.0 ± 2	−2.30	326
−0.0006 ± 0.00005	303.0 ± 2	293.0 ± 2	−2.65	329
−0.0008 ± 0.00005	225.0 ± 2	225.0 ± 2	−3.05	337
−0.0010 ± 0.0001	178.0 ± 1	178.0 ± 1	−3.33	346

Since in this region the carrier density is constant, this gives for the mobility a dependence

$$\mu = CT^{-2.0} \tag{3.18}$$

which is in disagreement with the prediction of Eq. 3.7. It is, however, the correct value for germanium, indicating that the simplified calculations used in deriving Eq. 3.7 are not completely adequate.

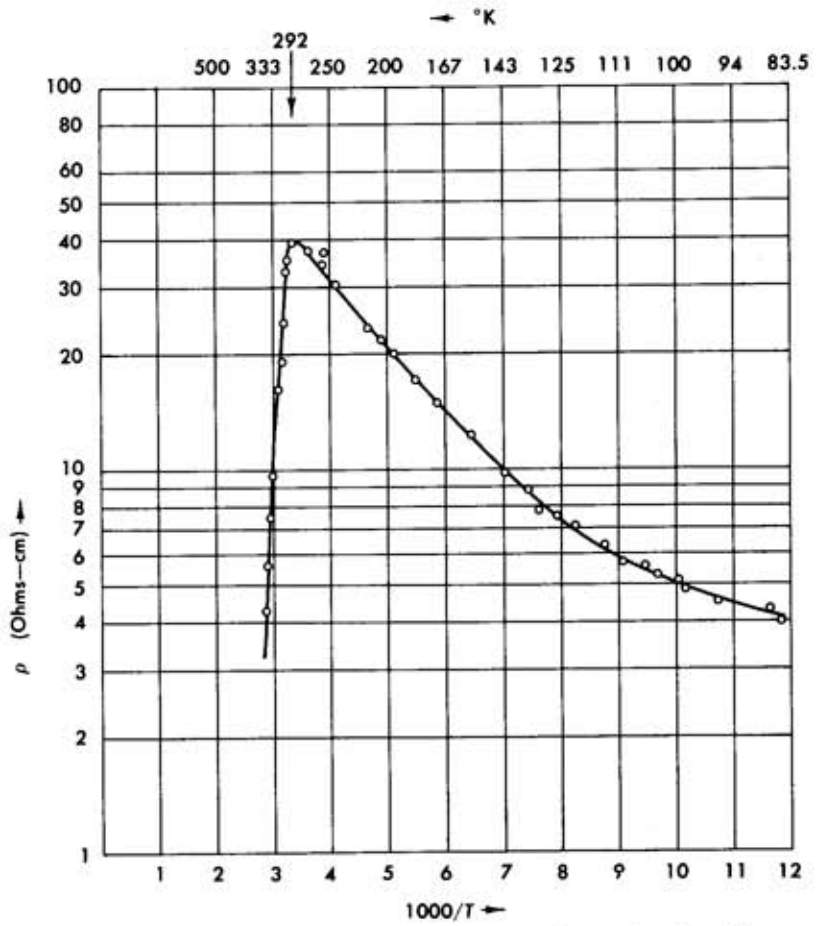

FIG. 3.25 The resistivity of a pure germanium crystal as a function of inverse temperature. For $T < 290°$ K, conduction is due mainly to the impurity carriers (extrinsic region); for $T > 290°$ K, conduction is due to electrons transferred to the conduction band (and the corresponding holes created in the valence band): this is the intrinsic region.

Turning now to the Hall-voltage measurements of Table 3.2, we can form the quantities defined by Eq. 3.8c.

$$\frac{V_H}{V_S} = \phi = \mu H \frac{t}{l}$$

hence

$$R_H = \phi R \frac{w}{H}$$

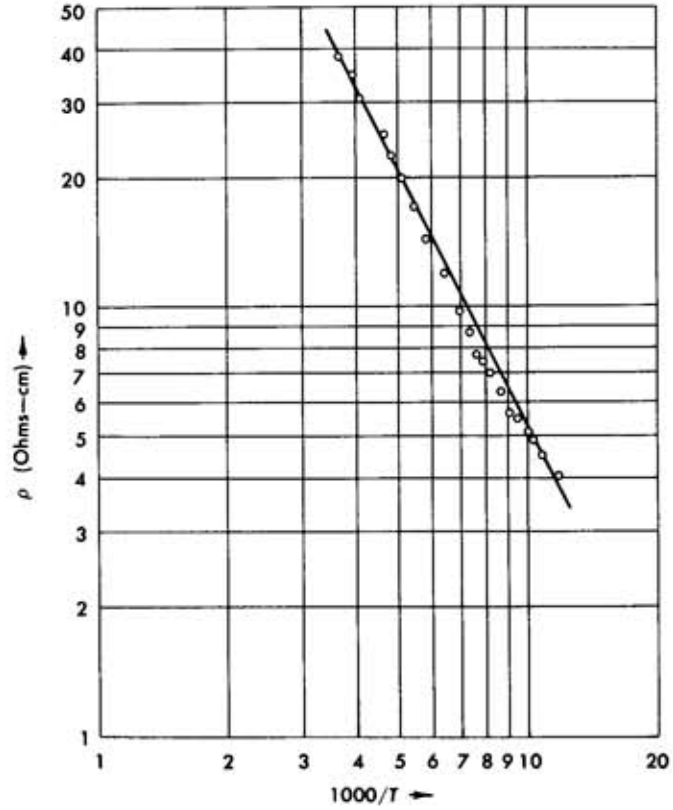

FIG. 3.26 A log-log plot of the resistivity of germanium in the extrinsic region versus $1/T$. It is assumed that the number of carriers is independent of T since saturation of the impurity carriers has already been reached.

and the Hall mobility

$$\mu_H = R_H\sigma = \phi\left(\frac{l}{t}\right)H^{-1}$$

The Hall mobility so obtained is shown in a log-log plot against T in Fig. 3.27. Since the Hall coefficient changes sign, we can immediately recognize that the crystal is of the p type; the inversion temperature of this particular sample is found to be

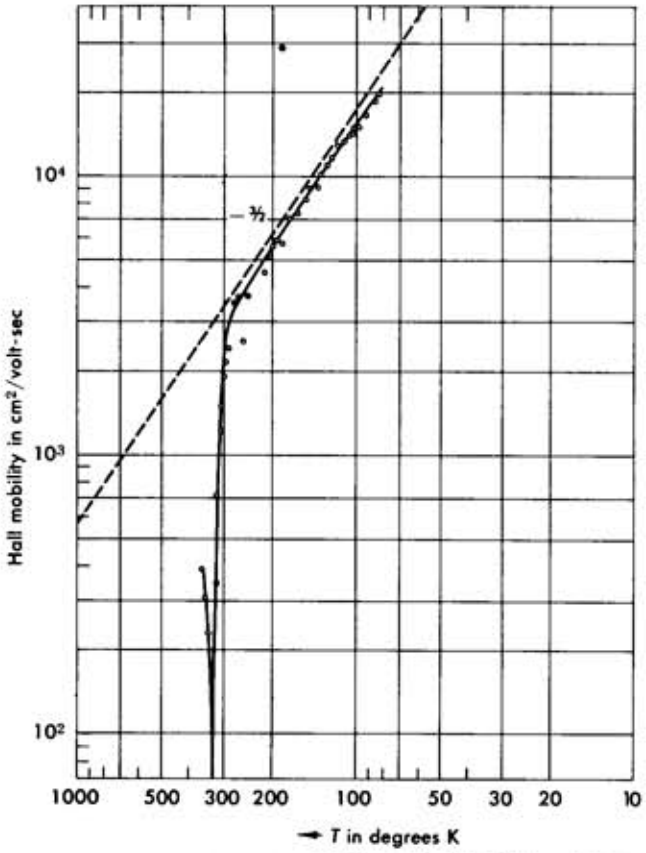

FIG. 3.27 Log-log plot of the "Hall-mobility" (Hall coefficient × conductivity) versus T. We note that the Hall coefficient becomes zero at $T = 323°$ K (inversion temperature) and changes sign beyond that point. Since negative values cannot be shown on the log plot for $T > 323°$ K, the Hall mobility of the reverse sign is again shown in the same graph. Note also the $T^{-3/2}$ dependence of the Hall mobility in the extrinsic region.

$$T_0 = (323 \pm 3)° \text{ K}$$

From the slope of the μ_H curve in the extrinsic region in Fig. 3.27, we obtain

$$\mu_H = CT^{-3/2} \tag{3.19}$$

which is different from Eq. 3.18 and is in agreement with conclusions of other observers; this is the reason why a distinction between the Hall mobility μ_H and the drift mobilities μ_D obtained from resistivity measurements is made.

By extrapolating Eq. 3.19 to the inversion temperature, we obtain the hole mobility† at $T = T_0 = 323°$;

$$\mu_H(h) = 2.7 \times 10^3 \text{ cm}^2/\text{V-sec}. \tag{3.20a}$$

We can now apply the analysis indicated in Section 3.4, which led to Eq. 3.11. From Fig. 3.25 we have $R_e(T = T_0) = 2150$ ohms and $R_0 = 500$ ohms leading to $b = 1.31 \pm 0.2$. Thus we obtain for the electron mobility at $T = T_0 = 323°$

$$\mu_H(e) = 3.5 \times 10^3 \text{ cm}^2/\text{V-sec}, \tag{3.20b}$$

both results being in agreement with the accepted values.

From the Hall coefficient in the extrinsic region, we can also obtain an order of magnitude for the density of impurity carriers. Since in that region only one type of carrier is present, $ne = 1/R_H$, and since

$$R_H = \frac{\phi Rw}{H} \simeq 8 \times 10^5 \text{ cm}^3/\text{coulomb}$$

$$n \simeq 8 \times 10^{12}/\text{cm}^3 \tag{3.21}$$

which is reasonable for this sample, indicating an impurity concentration of the order of two parts in 10^{10}.

From the data of Table 3.2 it can be further noticed that the resistance of the sample changes when the magnetic field is turned on. This phenomenon, called magnetoresistance, is due to the fact that the drift velocity of all carriers is not the same. With the magnetic field on, the Hall voltage $V = E_y l = |\mathbf{v} \times \mathbf{H}|$ compensates exactly the Lorentz force for carriers with the *average* velocity; slower carriers will be overcompensated, and faster ones undercompensated, resulting in trajectories that are not along the applied external field. This results in an effective decrease of the mean free path and hence an increase in resistivity.

† Note that 1 gauss = 10^{-4} weber/m² = 10^{-8} V-sec/cm².

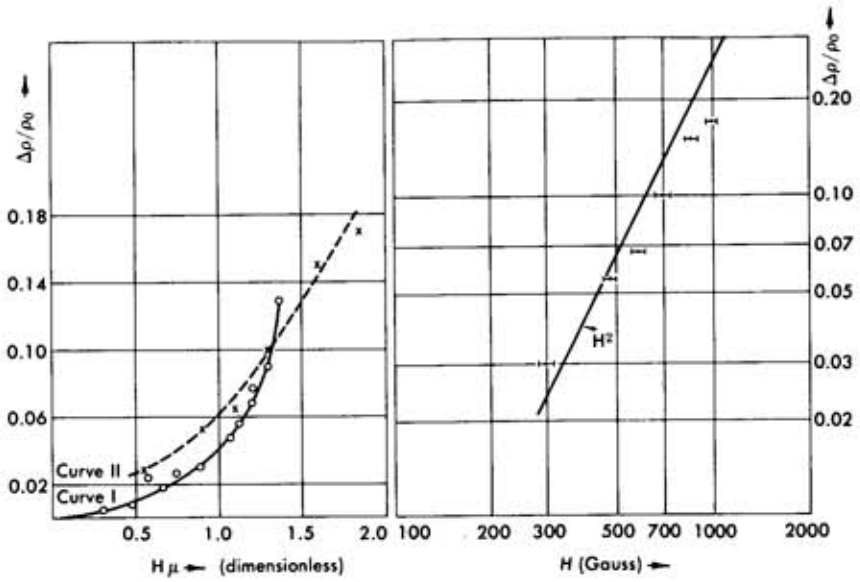

FIG. 3.28 Magnetoresistance of a germanium crystal; we plot $\Delta\rho/\rho_0 = (R_m - R)/R$ where R_m is the sample resistance with the field on, and R with field off. (a) A linear plot of $\Delta\rho/\rho_0$ versus the dimensionless parameter $H\mu_B$; curve I is obtained by varying μ at fixed H while curve II is obtained by varying H at fixed μ ($T = 84°$ K). (b) Log-log plot of $\Delta\rho/\rho_0$ versus H; note the H^2 dependence.

Several calculations of magnetoresistance have been made, but it is known that germanium in the extrinsic region exhibits many times the calculated value. One expects the magnetoresistance to increase with increased mean free path, and to reach saturation at very strong fields; for lower fields it is expected to have a quadratic dependence on the field strength. For the same reason, the Hall coefficient also has a slight dependence on magnetic field. Magnetoresistance measurements are of value in determining the exact shape of the energy surfaces.

Fig. 3.28 shows a plot of $\Delta\rho/\rho_0 = (R_m - R)/R$ (where R is the sample resistance without field, and R_m with magnetic field) obtained from the data of Table 3.2. In Fig. 3.28a, $\Delta\rho/\rho_0$ is plotted against the dimensionless parameter† $\mu H = eH\lambda(12\, m^*kT)^{-1/2}$. The points on curve I have been obtained by keeping H fixed and varying the temperature (hence μ). Curve II is obtained by varying H at a fixed $T = 84°$ K; the points from this curve are also shown on Fig. 3.28b, which is a log-log plot of $\Delta\rho/\rho_0$ against H, showing the almost quadratic dependence.

† See Eq. 3.8c.

4. Sketch of $p-n$ Semiconductor Junction Theory

As mentioned before, semiconductor materials with high impurity concentration, when properly combined, form a transistor. Transistors (of the type most used today) consist of two junctions of dissimilar-type semiconductors, one p type and one n type; the intermediate region, the base, is usually made very thin. We will briefly sketch the behavior of such a p-n junction and then see how the combination of two junctions can provide power amplification; for this we will use our knowledge of the band structure of semiconductors and the position of the Fermi level, as developed previously (Figs. 3.18 and 3.19).

When two materials with dissimilar band structure are joined, it is important to know at what relative energy level one band diagram lies with respect to the other: the answer is that *the Fermi levels of both materials must be at the same energy position* when no external fields are applied; this is shown in Fig. 3.29.

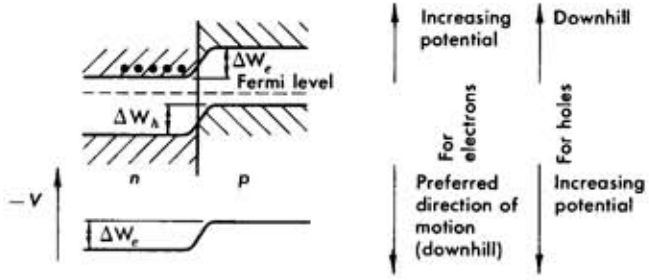

FIG. 3.29 Structure of the energy bands at the junction of an n-type and a p-type semiconductor.

From the energy diagram of the figure, it follows that only electrons with $E_e > \Delta W_e$ will be able to cross the junction from the n material into the p region and only holes with $E_h > \Delta W_h$ from the p region to the n region. Holes in the n region or electrons in the p region are called "minority carriers." Indeed, there will be diffusion of some minority carriers across the junction, but since no electric field is present these carriers will remain in the vicinity of the junction.†

If now a *reverse bias* is applied—that is, one that opposes the further motion of the minority carriers—the Fermi levels will become displaced by the amount of the bias, as shown in Fig. 3.30a. We see that the barriers

† The result of such diffusion is the build-up of a local charge density, and thus potential, which prevents further diffusion. Throughout the present analysis, however, we will neglect the local effects at the junction.

ΔW_e and ΔW_h are increased by almost the full voltage, making any motion of minority carriers across the junction very improbable. Fig. 3.30b, on the other hand, shows the situation when *forward bias* is applied (favoring the motion of minority carriers). The Fermi levels are now displaced in the opposite direction so that the barriers are lowered. However, the full bias voltage does not appear as a difference between the Fermi levels because dynamic equilibrium prevails. There is a continuous flow of minority carriers in the direction of the electric field (holes obviously moving in the opposite direction from electrons) and as a result a potential gradient exists along the material; thus the entire bias voltage does not necessarily appear at the junction itself.

We will now consider two junctions put together; in Fig. 3.31a, p-type, n-type, and again p-type material are joined. When no bias is applied, we expect the Fermi levels to be at the same position, with the resulting configuration shown in the diagram; in agreement with our previous conclusions from the consideration of a simple junction, we see that barriers exist for the motion of holes from the p regions into the n region, and also for the motion of electrons from the n region into either of the p regions.

Figure 3.31b shows the double junction under operating biases; note that one junction is biased *forward*, the other is biased in the *reverse* direction. The n-type material common to both junctions is called the *base*, while the p type of the forward-biased junction is the *emitter*; the p-type material of the reverse junction is the *collector*. A completely symmetric device consisting of n-p-n materials will perform similarly when the biases are reversed. From the energy diagram of Fig. 3.31b we can see that by varying the emitter junction bias we can control the injection of minority carriers into the base region; if the base region is made thin, it is possible for these holes to reach the collector junction, at which point they will immediately cross it, since it represents a gain in potential energy. If h_E is the minority carrier current injected into the base over a potential barrier $\Delta W_h(EB)$, the power required for injection is $P_{\text{in}} = h_E \, \Delta W_h(EB)$; similarly if h_C is the hole current into the collector down a potential drop $\Delta W_h(BC)$, the power gained is $P_{\text{out}} = h_C \, \Delta W_h(EC)$. Thus if $P_{\text{out}} > P_{\text{in}}$, the device is a power amplifier; since usually $\Delta W(CB) \gg \Delta W(EB)$, it suffices for $h_C \backsim h_E$ to give power gain.

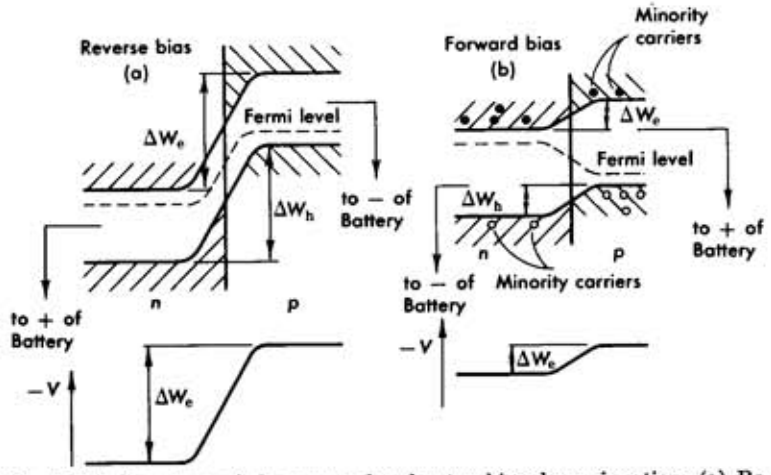

FIG. 3.30 Structure of the energy bands at a biased n-p junction. (a) Reverse bias. (b) Forward bias. The solid dots represent electrons, whereas the open dots holes.

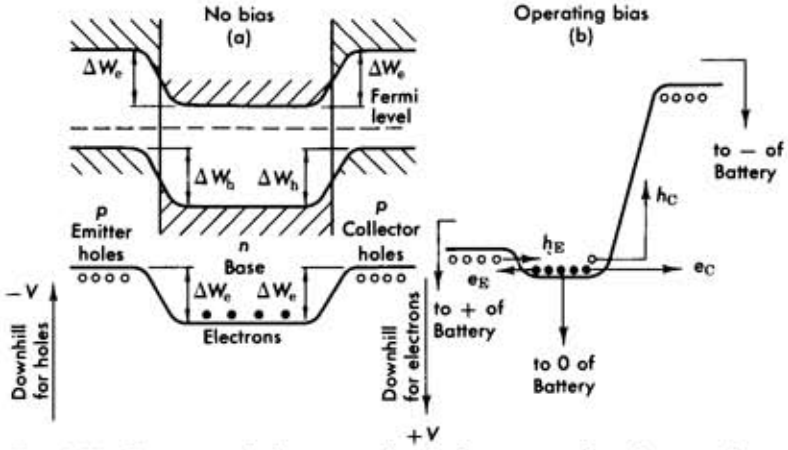

FIG. 3.31 Structure of the energy bands for a p-n-p junction transistor. (a) With no bias applied. (b) With operating biases. Note that the emitter is forward biased whereas the collector is reverse biased.

Below we give, without proving, some quantitative formulas for the gain factors of a junction transistor. A detailed discussion can be found in Dunlap, "*An Introduction to Semiconductors.*"

We introduce the following symbols and definitions:

h_E, e_E	hole current out of emitter, electron current into emitter
h_C, e_C	hole current, electron current into collector
I_E, I_B, I_C	emitter, base, collector current where hole current *leaving* a region is designated as positive
w	width of base region
D_n, D_p	diffusion coefficients for electrons, holes in base region
L_E, L_B	diffusion lengths in emitter, base
t_E, t_B	lifetime of minority carriers in emitter, base
n_E, p_B	concentration of minority carriers (electrons) in emitter, (holes) in base
ω	angular frequency

i	$\sqrt{-1}$
β	h_E/h_C diminution factor
γ	h_E/I_E injection efficiency
α	I_C/I_E current gain

If h_E holes are injected from the emitter into the base, because of recombination, only h_C reach the collector junction. Thus:

$$h_C = h_E\beta$$

where $0 < \beta < 1$, and β is given by $\beta = \operatorname{sech}(w/L_B)$. Further

$$I_E = h_E + e_E = h_E\left(1 + \frac{e_E}{h_E}\right) = \frac{h_E}{\gamma}$$

where $0 < \gamma < 1$, and is given by

$$\frac{1}{\gamma} = 1 + \frac{e_E}{h_E} = 1 + \frac{D_n}{D_p}\frac{n_E}{p_B}\frac{L_B}{L_E}\tanh\left(\frac{w}{L_B}\right)$$

Also,

$$I_C = -h_C + e_C \qquad I_B = -e_C - e_E + (h_C - h_E)$$

with the obvious conservation expression

$$I_C = -(I_E + I_B)$$

Since the collector leakage current e_C is very small, we can neglect it and obtain

$$\alpha = \frac{I_C}{I_E} \simeq \frac{h_C}{I_E} = \frac{h_E\beta}{h_E/\gamma} = \beta\gamma$$

Usually $w/L_B \ll 1$ and then $\gamma \simeq 1$, so we obtain the further approximate expressions

$$\alpha \simeq \beta = \operatorname{sech}\left(\frac{w}{L_B}\right) \simeq \left[1 + \tfrac{1}{2}\left(\frac{w}{L_B}\right)^2\right]^{-1} \tag{4.1}$$

indicating the importance of a thin base region if current gains close to unity are to be achieved. For a time-varying signal with angular frequency ω, the above expression is modified to

$$\alpha \simeq \beta \simeq \left[1 + \tfrac{1}{2}(1 + i\omega t_B)\left(\frac{w}{L_B}\right)^2\right]^{-1} \tag{4.2}$$

indicating phase shifts and reduction of gain at frequencies of the order of the reciprocal lifetime of the minority carriers in the base.

References

For the material covered in Sections 3, 4, and 5 the reader may also consult the following texts:

W. C. Dunlap, Jr., *An Introduction to Semiconductors*. New York: Wiley, 1957. Brief but clear treatment.

C. Kittel, *Introduction to Solid State Physics*. New York: Wiley, 1953. A more general treatment of the solid state.

W. Shockley, *Electrons and Holes*. New York: D. Van Nostrand, 1950. A thorough presentation of the subject.

5. Contact and Thermoelectric Effects at Junctions of Metals

We now turn our attention again to metals; as mentioned in Sections 1 and 2, the free electrons can be thought of as being all in the continuum of the Fermi sea, with the density of states proportional to $\sqrt{E}$ and not restricted to allowed energy bands. If two metals with different Fermi energies $w_F(A)$ and $w_F(B)$ and different work functions $\phi(A)$ and $\phi(B)$ are joined, the energy diagram will be as shown in Fig. 3.32. Again equilibrium requirements impose the condition that the Fermi levels be at the same potential.

Let us consider, then, an electron in metal B that just overcomes the work function ϕ_B and is emitted from the metal surface. If while outside the metal the electron moves towards the dissimilar metal A (which is joined to B), it clearly sees a retarding potential $\phi_A - \phi_B$ until it enters metal B. This is called the *contact potential*; note that we had to correct for it on several occasions in discussions in Chapter 1. For an electron emitted from A and traveling towards B, the contact potential is an accelerating one ($\phi_B - \phi_A$). Thus we see that contact potential differences (cpd) arise when current flow through dissimilar metals is completed with a section in free space.

Next we will briefly mention three interrelated phenomena connecting the *reversible* flow of heat with that of current in a metal and vice versa. An application of these effects is the thermocouple of which we have repeatedly made use.

(a) *The Peltier effect* (1834): Let a circuit be completed through two dissimilar metals and a current flow through the junction. Reversible (not Joule) heating or cooling of the junction then occurs depending on the

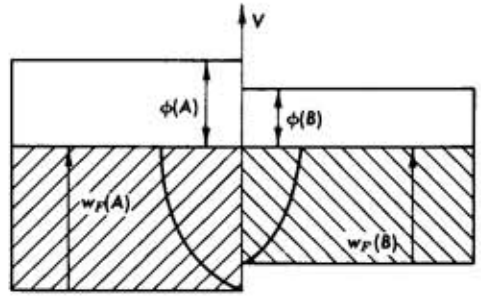

FIG. 3.32 The junction of two dissimilar metals, with different work functions and different potential barriers. Note that the Fermi levels of both metals are at the same energy. The contact potential differences equal $\phi_A - \phi_B$.

direction of current flow. Analytically we express the effect as follows

$$Q = \pi_{AB}(T)q \tag{5.1}$$

where Q is the amount of heat liberated, q is the total charge that crosses the junction, and $\pi_{AB}(T)$ is the Peltier coefficient which depends on the temperature.

(b) *The Thomson effect* (1856): This is complementary to the Peltier effect and is the reversible heating or cooling of a conductor through which current flows and along which a temperature gradient exists. Consider a conductor AB with no current flowing but with its two end points at a different temperature $T_A > T_B$; there will be heat transfer across it, effected through the motion of high-energy electrons from A towards B; to keep the charge transfer equal to zero, low-energy electrons will move from B towards A: this is shown in Fig. 3.33a. The following must hold

$$j = e(n_2v_2 - n_1v_1) = 0 \tag{5.2a}$$

and if S is the rate of heat transfer and $E_2 = E_A - \hat{E}$, $E_1 = \hat{E} - E_B$ are the excess or deficit from the mean thermal energy,

$$\frac{\Delta Q}{\Delta t} = (n_2v_2E_2 + n_1v_1E_1) = S \tag{5.3a}$$

If now a net current flows to the right (Fig. 3.33b),

$$j' = e(n_2'v_2' - n_1'v_1') > 0 \tag{5.2b}$$

and

$$\frac{\Delta Q}{\Delta t} = n_2'v_2'E_2 + n_1'v_1'E_1 = S' \neq S \tag{5.3b}$$

Namely, a change in $\Delta Q/\Delta t$ occurs; the balance of the heat is being supplied

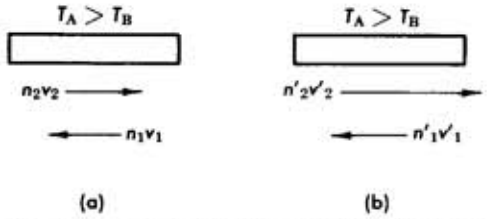

FIG. 3.33 A conductor along which a temperature gradient exists. (a) No net current flowing. (b) Current flowing to the right.

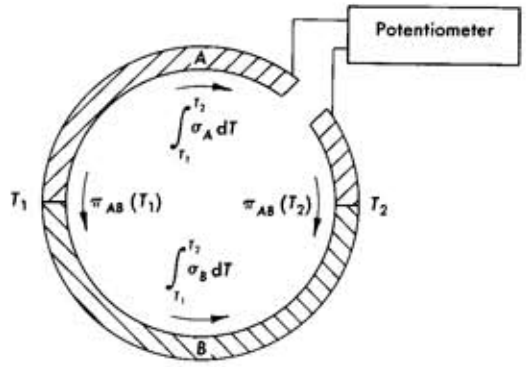

FIG. 3.34 A thermocouple made of two dissimilar metals A and B. Note that the two junctions are at different temperatures T_1 and T_2 and that there is no net current flow. The two effects contributing to the thermoelectric electromotive force are shown.

or absorbed by the lattice. The situation is reversed when the current flows to the left.

Analytically, we express the Thomson effect as follows:

$$\frac{dQ}{dx} = \sigma_A\, q \left(\frac{dT}{dx}\right) \tag{5.4}$$

where dQ/dx is the heat absorbed (or liberated) per unit length of the metal; q is the total electric charge that has flowed through, and dT/dx the temperature gradient; finally σ_A is the Thomson coefficient and it depends on the metal. Conversely if a temperature gradient exists in a metal, an electromotive force (emf) will appear at its ends. Since the product of the charge and of the electromotive force must equal the total work done, we find by integrating Eq. 5.4

$$\int_A^B dQ = q \int_{T_A}^{T_B} \sigma_A\, dT$$

hence

$$\text{emf (Thomson)} = \int_{T_A}^{T_B} \sigma_A\, dT \tag{5.5}$$

(c) *The Seebeck effect* (1822): This is the appearance of an electromotive force in a circuit made of two dissimilar metals when their junctions are held at different temperatures—namely, a thermocouple. It has to be a combination of the two previously discussed effects and is shown in Fig. 3.34. The two metals will have dissimilar Thomson coefficients σ_A and σ_B, and the junctions (at different temperature) will have dissimilar Peltier coefficients; the electromotive force is usually measured with

a potentiometer—namely, at zero current. Combining Eqs. 5.1 and 5.5 we obtain

$$\text{emf} = \pi_{AB}(T_2) - \pi_{AB}(T_1) + \int_{T_1}^{T_2} \sigma_A \, dT - \int_{T_1}^{T_2} \sigma_B \, dT \qquad (5.6)$$

Taking the derivative with respect to the temperature, we obtain the *thermoelectric power*, E_{AB} of two dissimilar metals

$$E_{AB} = \frac{d(\text{emf})}{dT} = \frac{d[\pi_{AB}(T)]}{dT} + (\sigma_A - \sigma_B) \qquad (5.7)$$

4

USEFUL TECHNIQUES

1. Introduction

This chapter deals with techniques that are needed repeatedly in many experiments. While the material presented is not exhaustive it is of such a nature that it is best presented by itself, detached from specific physical experiments.

The first topic is switching circuits, since they form the basic blocks of all counting and shaping circuits used with particle detectors; moreover they are the basis of all digital logic devices such as high-speed computers. Transistors, rather than vacuum tubes, are used as switching elements. This is followed by a brief mention of electronic functional assemblies to show how the basic blocks can be put together to perform logic functions.

Next, a section on means of creating and measuring vacuum is included. For most experiments in atomic or nuclear physics a good vacuum is needed, so that it is worthwhile to discuss the capabilities and limitations of modern vacuum equipment.

Finally, a discussion of radioactive safety and handling of radioactive materials is presented. This topic has been included because in many of the following experiments, especially those on nuclear physics, the student